Measuring viscosity with nonlinear self-excited microcantilevers

Cite as: Appl. Phys. Lett. **111**, 144101 (2017); https://doi.org/10.1063/1.4995386
Submitted: 11 July 2017 • Accepted: 22 September 2017 • Published Online: 03 October 2017

J. Mouro, B. Tiribilli and P. Paoletti

Measuring viscosity with nonlinear self-excited microcantilevers

J. Mouro,[1] B. Tiribilli,[2] and P. Paoletti[1]
[1]*School of Engineering, University of Liverpool, Brownlow Hill, Liverpool L69 3GH, United Kingdom*
[2]*Institute for Complex Systems, National Research Council (ISC-CNR), via Madonna del Piano 10, Sesto Fiorentino, Firenze I-50019, Italy*

(Received 11 July 2017; accepted 22 September 2017; published online 3 October 2017)

A viscosity sensor based on the nonlinear behaviour of a microcantilever embedded in a self-excitation loop with an adjustable phase-shifter is proposed. The self-sustained oscillation frequencies of the cantilever are experimentally and theoretically investigated as functions of the fluid viscosity and of the imposed phase shift of the signal along the self-excitation loop. The sensor performance is validated experimentally using different water-glycerol solutions. In contrast to existing rheological sensors, the proposed platform can be tuned to work in two different modes: a high-sensitivity device whose oscillation frequency changes smoothly with the rheological properties of the fluid or a critical viscosity threshold detector, where, for small changes in fluid viscosity, there is a step change in oscillation frequency. https://doi.org/10.1063/1.4995386

Micromechanical resonators have been proposed as promising mass or rheological sensors, capable of unprecedented sensitivities and operating with extremely small volumes of fluid.[1,2] However, the standard external excitation of these sensors vibrating in viscous fluids is typically associated with low quality factors (Q) and the presence of undesired vibration modes.[3,4] More recently, strategies where a microresonator is embedded in a feedback loop proved to be very effective in mitigating these limitations and in achieving a more selective frequency response of the resonator. These feedback strategies include the use of self-excitation circuits[5,6] or parametric resonance,[7,8] which allowed the use of a microresonator for imaging[6,9] or as a mass sensor.[10] One of the main drawbacks of the feedback loop approaches is the presence of multiple sources of nonlinearities,[1,2,9–11] which can cause poorly understood phenomena. In particular, it has been highlighted that the microcantilever dynamic response is strongly affected by the delay present in the feedback loop.[12–14]

In this work, it is shown how the nonlinear dynamics of a cantilever embedded in a feedback loop with an adjustable phase-shifter can be used as a high-sensitivity or threshold rheological sensor. The frequencies of the oscillations in the feedback loop are studied as a function of the viscosity of different water-glycerol solutions and the delay that is introduced in the loop by the phase-shifter.

A schematic of the experimental setup is shown in Fig. 1(a). The cantilever motion is acoustically excited using a dither piezo, and the resulting deflection is measured using a four-quadrant detector connected to a R9 controller (RHK Technology). The measured deflection is fed to an electronic circuit (Elbatech srl) composed of an adjustable phase-shifter, a gain, and a saturator. The output voltage of these elements is connected to the dither piezo. The deflection signal is also fed to a spectrum analyser embedded in the R9 controller to measure the oscillation frequency of the cantilever. The configuration shown in Fig. 1(a) induces self-sustained stable oscillations of the cantilever. These oscillations result from the balance between the feedback gain, which constantly amplifies the motion of the cantilever (inducing unstable exponentially growing trajectories), and the nonlinear saturation, which limits the system trajectories and stabilizes the system dynamics on stable self-sustained oscillations with a certain frequency and amplitude.[5,14] The frequency and amplitude of the oscillation guarantee that the gain of the loop is unitary and that the total phase shift around the feedback loop is an integer multiple of 2π radians.[14,15]

The total delay τ_{tot} [indicated in Fig. 1(a)] accounts for the intrinsic delay due to the propagation of the electrical signals across the electronic components and to elastic waves in the cantilever and probe holder materials. In addition to this delay, the adjustable phase-shifter that is inserted in the loop [detailed in Fig. 1(b), with the respective transfer function] allows users to shift the phase between the dither piezo excitation and the cantilever deflection by adjusting the potentiometer R_2. The phase shift induced by the phase-shifter is, at most, π radians. Finally, the polarity of the voltage applied to the terminals of the dither piezo can also be inverted [$p = \pm 1$, Fig. 1(a)], allowing an additional phase shift of π radians to the signal. A more detailed description of this setup is reported in Ref. 14.

In conclusion, the sweep of the values of R_2, added to the inversion of polarity in the piezo, allows the signal along the loop to be shifted by a complete oscillation period (2π radians) in a controlled manner. The total phase shift around the feedback loop must be an integer multiple of 2π radians for self-sustained oscillations to exist.[14,15] Therefore, the cantilever will naturally adjust its phase (and hence its oscillation frequency) to compensate for the overall phase imposed by the adjustable phase-shifter, the fixed polarity, and the intrinsic total delay of the setup.

For the experiments, two cantilevers (ACST by AppNano and CLFC-A by Bruker) were immersed in eight water-glycerol solutions with different viscosities {ranging

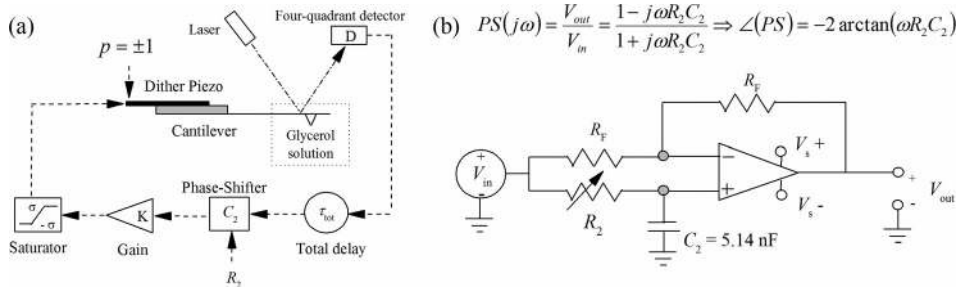

FIG. 1. (a) Schematic of the experimental setup. The deflection signal of the cantilever vibrating in water-glycerol solutions passes through the phase-shifter, gain, and saturator of the feedback loop and is fed back to the excitation piezo as a voltage. (b) Architecture of the phase-shifter and its transfer function. The shift imposed by the phase-shifter in the loop is $\angle(PS(\omega)) = -2a\tan(\omega R_2 C_2)$, where ω is the loop self-oscillation frequency.

from pure water, $\eta \approx 0.0010\,Pa\,s$, to G_{50} [solution of 50% (v/v)], $\eta \approx 0.0084\,Pa\,s$, at room temperature (20 °C)[16], and the loop self-oscillation frequencies were recorded, while the value of the potentiometer R_2 was systematically reduced from 10.12 to 0 kΩ. The polarity on the terminals of the piezo was then inverted, and the sweep of R_2 was repeated, while recording the probe oscillation frequency.

Figure 2 presents the experimental results for the case where R_2 is systematically reduced while operating in solutions of fixed viscosity. The self-oscillation frequencies of cantilever CLFC-A in the water-glycerol solutions are shown as a function of the value of the potentiometer R_2 for the two polarities applied on the piezo. The left panel shows the case of the non-inverted polarity ($p = 1$), where the sweep of R_2 causes the cantilever phase to move in the interval $[0, -\pi]$ radians. It can be observed that the oscillation frequencies are weakly affected by changes in R_2 (and, consequently, in the cantilever phase) but strongly dependent on the viscosity of the fluid. For high values of R_2, there is a steep continuous increase in the oscillation frequencies and the dependence on the fluid viscosity collapses.

When the polarity on the piezo is inverted ($p = -1$, right panel), the cantilever phase is forced to move in the interval $[-\pi, -2\pi]$ radians. In this case, no clear dependence on the fluid viscosity is observed, but a sudden transition from low to high oscillation frequencies occurs for specific values of R_2.[14] The inset highlights that this sudden transition occurs at distinct values of R_2 in water and G_{15} solutions. The cantilever phase depends on the viscosity of the medium, and therefore, the phase-shifter needs to impose different shifts in the loop in order to achieve the required phase shift of 2π radians (refer to the supplementary material for further details).

The results shown in Fig. 2 suggest the possibility of using this platform in two different modes: first, as a *continuous* viscosity sensor, where different fluid viscosities induce a measurable shift of the oscillation frequency (left panel) and second, as a *threshold* viscosity sensor, where the oscillation frequency suddenly transitions for small changes of the phase in the loop (right panel).

These two modes are illustrated in Fig. 3, where the oscillation frequencies of the self-excited probe are plotted against the viscosity of the media,[16] for the case of non-inverted polarity [Fig. 3(a), *continuous* sensor] and inverted polarity [Fig. 3(b), *threshold* sensor]. Figure 3(a) shows that the oscillation frequencies of the loop decrease with the viscosity of the medium, for constant values of potentiometer R_2. Conversely, Fig. 3(b) shows that far from the sudden transition (green circles, $R_2 = 4.0$ kΩ), the oscillation frequencies are independent of fluid viscosity (in accordance with the right panel of Fig. 2). More interestingly, close to the transition region, the oscillation frequency of the system immersed in G_5 can be at either side of the transition (high or low frequencies), depending on the chosen value of R_2. As the transition location depends on the viscosity of the medium (as seen in the inset of Fig. 2), given a certain critical value of viscosity, the sensor could be tuned (by R_2) to oscillate very close to the transition point so that even a small alteration in viscosity will trigger the transition, producing a sharp change in oscillation frequency.

The experimental results, discussed above, were modelled using two alternative strategies. First, the equation of motion of the cantilever in the feedback loop is numerically simulated in the time domain using *Simulink*, as detailed in Ref. 14. The second strategy (described in detail in the

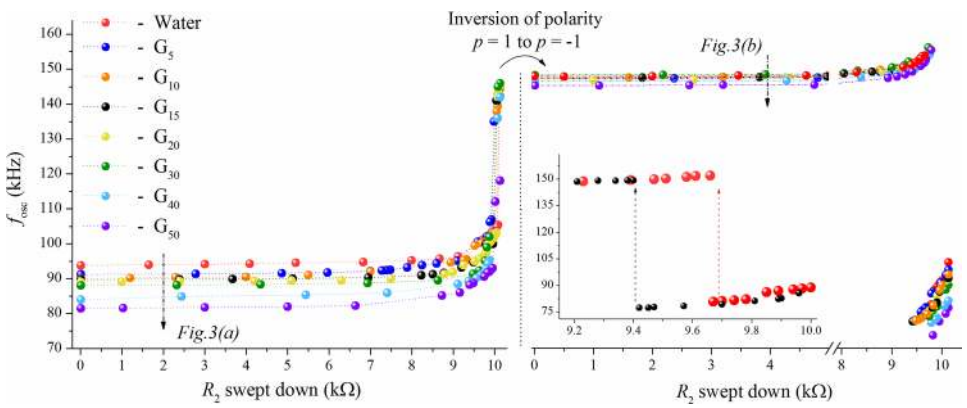

FIG. 2. Oscillation frequency of cantilever CLFC-A as a function of the fluid viscosities and values of R_2, for two different polarities. Left: dependency on fluid viscosity. Right: sudden transition of the oscillation frequency at a particular value of R_2. The dashed arrows indicate cuts of constant R_2, as presented in Fig. 3.

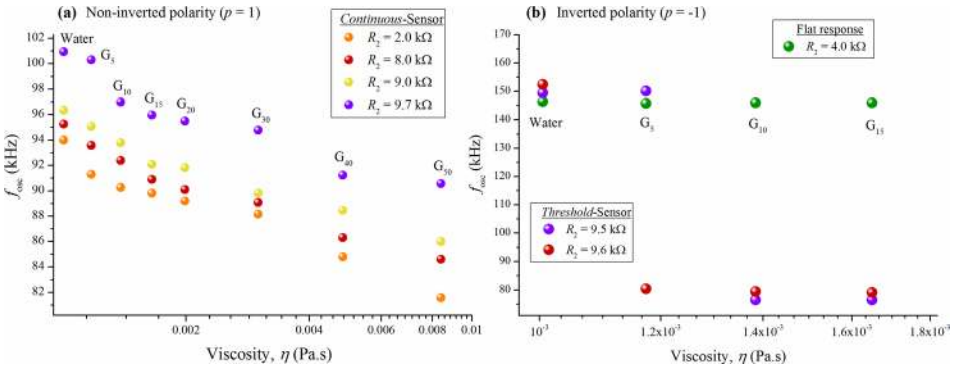

FIG. 3. Two types of viscosity sensors in cantilever CLFC-A. (a) *Continuous*-sensor, where the oscillation frequency depends on the fluid viscosity. (b) *Threshold*-sensor, where the sudden transition in oscillation frequency can be used to monitor small changes in viscosity. The concentration of each solution is indicated near the corresponding symbols.

supplementary material) is a frequency domain approach which analytically solves the phase condition for the existence of self-sustained oscillations in the loop. In both strategies, the cantilever is modelled as a harmonic oscillator subjected to Sader's hydrodynamic forcing.[17–19]

Figure 4 presents a set of experimental and modelled results for the ACST cantilever. The top panels show the measured oscillation frequencies of the ACST cantilever immersed in different water-glycerol solutions as a function of R_2 and p. Two regimes are shown for the case of the *continuous*-sensor [Fig. 4(a), non-inverted polarity] and *threshold*-sensor [Fig. 4(b), inverted polarity].

The symbols represent the measured experimental data, while the dashed-dotted lines show the results from the *Simulink* model. The inset in Fig. 4(b) highlights how the location of the transition depends on the viscosity of the medium. The dynamic *Simulink* model captures the experimentally observed behaviour, both in the *continuous* and the *threshold* mode. The values of viscosity and density of the solutions (from Ref. 16) are required as inputs to the model, together with the measured value for the total delay $\tau_{tot} = 9.5\ \mu s$ (detailed in Ref. 14).

The second modelling strategy finds an analytical dependence between the cantilever oscillation frequency in the feedback loop and the viscosity of the medium, for each fixed set of experimental conditions (values of R_2 and τ_{tot}). The lines plotted in the bottom panels of Fig. 4 correspond to solutions of the following equation:

$$\sqrt{\eta} = \frac{-Y \pm \sqrt{Y^2 + 4XZ}}{2X}, \tag{1}$$

where $X = Lf_{osc}b_2\pi^2$, $Y = (b_1 - a_2x)LW\sqrt{{f_{osc}}^3\pi^5\rho}$, and $Z = -xk + x(2\pi f_{osc})^2\left(m + \frac{\pi}{4}\rho LW^2a_1\right) - 2\pi f_{osc}c$. In these expressions, η and ρ are the fluid viscosity and density, and a_1, a_2, b_1, and b_2 are constants used to describe the hydrodynamic force.[17–19] The cantilever geometry is represented by its width W and length L. The dynamical response of the probe is characterized by m, k, and c which represent the cantilever mass, spring constant, and intrinsic damping coefficient. Finally, f_{osc} is the self-sustained oscillation frequency, and $x = \tan(\varphi_{ct})$, where φ_{ct} is the phase of the cantilever working in the feedback-loop and depends on the total phase shift introduced by the phase-shifter and total delay of the system. The detailed derivation of this analytical equation is reported in the supplementary material. Only real and positive values of η are considered when plotting Eq. (1). It is worth noting the similarity of these curves with the experimental data shown in Fig. 3.

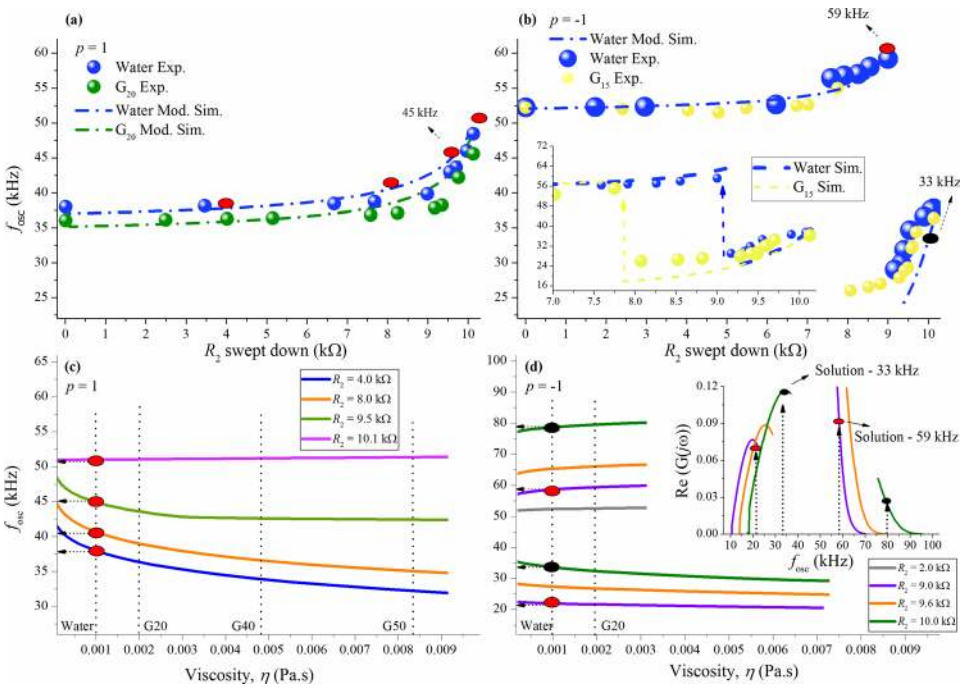

FIG. 4. Top panels: experimental and *Simulink* predicted results for the cantilever ACST. (a) Region of the *continuous*-sensor. (b) Region of the *threshold*-sensor. Bottom panels: plots of Eq. (1) for the self-sustained oscillation frequencies as a function of the fluid viscosity. (c) *Continuous*-sensor, $p = 1$. (d) *Threshold*-sensor, $p = -1$. Inset: real part of the transfer function, $G(j\omega) = pCT(j\omega)PS(j\omega)e^{-j\omega\tau_{tot}}$, used to identify the stable solution according to the Nyquist Stability Criterion.[14,20]

Figure 4(c) (bottom left) shows the plots of Eq. (1) for different fixed values of the potentiometer R_2 and non-inverted polarity, where the system acts as a *continuous*-sensor. There is a one-to-one dependence between the closed-loop oscillation frequency and the fluid viscosity. As shown in Fig. 4(c), fixing the value of viscosity of the water ($\eta \approx 0.0010\,\mathrm{Pa\,s}$[16]) and looking for the crossings with the plots of Eq. (1) (red circles), the oscillation frequencies of the system can be determined. These frequencies are then plotted in the upper panel [Fig. 4(a)—red circles, for the corresponding value of R_2] and show a good agreement with both the experimental data and the predicted results from the *Simulink* model. Note also that, for low values of R_2, the plots of Eq. (1) are convex, meaning that the oscillation frequency decreases with the increase in viscosity, as expected and observed experimentally in this region [see Fig. 3(a)]. For high values of R_2, the plots become slightly concave (purple curve, for $R_2 = 10.1\,\mathrm{k\Omega}$) and the oscillation frequency becomes almost insensitive to the fluid viscosity. This trend was also observed experimentally in Fig. 3(a).

Figure 4(d) (bottom right) presents the same curves for the inverted polarity case, where the system acts as a *threshold*-sensor. In this case, the oscillation frequency is a non-injective function of fluid viscosity, as, for example, the purple and green lines show two possible oscillation frequencies for each value of viscosity (black and red circles, respectively). However, as discussed in the supplementary material, the Nyquist Stability Criterion states that the stable solution has the highest real part of the transfer function $G(j\omega) = pCT(j\omega)PS(j\omega)e^{-j\omega\tau_{tot}}$.[14,20] The real part of this transfer function is calculated numerically and plotted within the inset of Fig. 4(d), showing that for $R_2 = 9\,\mathrm{k\Omega}$ (purple line, red circles), the stable solution occurs at 59 kHz, while for $R_2 = 10\,\mathrm{k\Omega}$ (green line, black circles), the stable solution is at 33 kHz. These points are plotted in Fig. 4(b) and agree with both the experimental observations and *Simulink* model results. The transition (where the real part of the transfer function of both solutions is equal) occurs for $R_2 = 9.6\,\mathrm{k\Omega}$ (orange lines).

In this work, the dependence of the oscillation frequency of a self-excited microcantilever is measured and modelled as a function of the fluid viscosity and the phase shift of the signal along the loop. This setup shows a high signal-to-noise ratio, as it does not involve any of the external frequency sweeps that are typically used to identify resonance. By tuning the phase of the cantilever (via the phase-shifter), the user can choose to employ the same device as a *continuous* sensor, where the oscillation frequency changes smoothly with the rheological properties of the fluid, or as a *threshold* detector, where the oscillation frequency rapidly transitions for small changes of viscosity. Such a degree of flexibility is not available with current microcantilever-based rheology sensors.

See supplementary material for a detailed mathematical derivation of Eq. (1).

The authors wish to acknowledge the support of EPSRC Grant No. EP/N026799/1 on Self-Tuning Advanced Rheology Tool and of the CNR Short Term Mobility grants 2015 and 2016. The authors also wish to thank Elbatech srl for the support in the design and realization of the self-excitation electronics. The data presented in this paper are freely available at https://doi.org/10.5281/zenodo.825797.

[1]D. Ossola, P. Dorig, J. Voros, T. Zambelli, and M. Vassalli, Nanotechnology **27**, 415502 (2016).
[2]N. Belminoud, I. Dufour, A. Colin, and L. Nicu, Appl. Phys. Lett. **92**, 041907 (2008).
[3]T. E. Schaffer, J. P. Cleveland, F. Ohnesorge, D. A. Walters, and P. K. Hansma, J. Appl. Phys. **80**, 3622 (1996).
[4]A. Labuda, K. Kobayashi, D. Kiracofe, K. Suzuki, P. H. Grütter, and H. Yamada, AIP Adv. **1**, 022136 (2011).
[5]M. Basso, P. Paoletti, B. Tiribilli, and M. Vassalli, Nanotechnology **19**, 475501 (2008).
[6]M. Basso, P. Paoletti, B. Tiribilli, and M. Vassalli, IEEE Trans. Nanotechnol. **10**(3), 560 (2011).
[7]G. Prakash, S. Hu, A. Raman, and R. Reifenberger, Phys. Rev. B **79**, 094304 (2009).
[8]G. Prakash, A. Raman, J. Rhoads, and R. Reifenberger, Rev. Sci. Instrum. **83**, 065109 (2012).
[9]L. Manning, B. Rogers, M. Jones, J. D. Adams, J. L. Fuste, and S. C. Minne, Rev. Sci. Instrum. **74**(9), 4220 (2003).
[10]S. Olcum, N. Cermak, S. C. Wasserman, and S. R. Manalis, Nat. Commun. **6**, 7070 (2015).
[11]W. J. Venstra, H. J. R. Westra, and H. S. J. van der Zant, Appl. Phys. Lett. **97**, 193107 (2010).
[12]R. van Leeuwen, D. M. Karabacak, H. S. J. van der Zant, and W. J. Venstra, Phys. Rev. B **88**, 214301 (2013).
[13]V. Zega, S. Nitzan, M. Li, C. H. Ahn, E. Ng, V. Hong, Y. Yang, T. Kenny, A. Corigliano, and D. A. Horsley, Appl. Phys. Lett. **106**, 233111 (2015).
[14]J. Mouro, B. Tiribilli, and P. Paoletti, J. Micromech. Microeng. **27**, 095008 (2017).
[15]R. M. C. Mestrom, R. H. B. Fey, and H. Nijmeijer, IEEE/ASME Trans. Mechatronics **14**(4), 423 (2009).
[16]See http://www.met.reading.ac.uk/~sws04cdw/viscosity_calc.html for density and viscosity of water-glycerol solutions.
[17]J. E. Sader, J. Appl. Phys. **84**(1), 64 (1998).
[18]A. Maali, C. Hurth, R. Boisgard, C. Jai, T. Cohen-Bouhacina, and J. P. Aimé, J. Appl. Phys. **97**, 074907 (2005).
[19]I. Dufour, A. Maali, Y. Amarouchene, C. Ayela, B. Caillard, A. Darwiche, M. Guirardel, H. Kellay, E. Lemaire, F. Mathieu, C. Pellet, D. Saya, M. Youssry, L. Nicu, and A. Colin, J. Sens. **2012**, 9.
[20]H. K. Khalil, *Nonlinear Systems*, 3rd ed. (Prentice-Hall, Upper Saddle River, NJ, 2002).